Microbial production of 3-hydroxypropionic acid by acetic acid bacteria: Modeling including the buffering capacity of the biological medium enables prediction of pH and metabolite concentrations

Pedro Arana-Agudelo, Florence de Fouchécour, Marwen Moussa, Violaine Athès, Kevin Lachin, Henry Eric Spinnler, Claire Saulou-Bérion, Ioan-Cristian Trelea

Biochemical Engineering Journal 208 (2024) 109346

Contents lists available at ScienceDirect

Biochemical Engineering Journal

journal homepage: www.elsevier.com/locate/bej

Regular article

Microbial production of 3-hydroxypropionic acid by acetic acid bacteria: Modeling including the buffering capacity of the biological medium enables prediction of pH and metabolite concentrations

Pedro Arana-Agudelo, Florence de Fouchécour, Marwen Moussa, Violaine Athès, Kevin Lachin, Henry-Eric Spinnler, Claire Saulou-Bérion, Ioan-Cristian Trelea *

Université Paris-Saclay, INRAE, AgroParisTech, UMR SayFood, Palaiseau F-91120, France

ARTICLE INFO

Keywords:
Acetobacter cerevisiae
Fed-batch bioconversion
Buffering capacity
Sensitivity analysis
Acid inhibition

ABSTRACT

A mathematical model of the fed-batch bioconversion of 1,3-propanediol into 3-hydroxypropionic acid using acetic acid bacteria is proposed. The model includes the microbial growth, the oxidation of 1,3-propanediol to 3-hydroxypropionaldehyde followed by a second oxidation reaction to 3-hydroxypropionic acid. The inhibitory effect of the total acid concentration upon the biological reactions was considered as well as the effect of pH on bacterial growth. A special attention was paid to make accurate pH predictions as pH is a key parameter that influences the microbial growth and bioconversion and also defines the strategy of downstream processing for acid recovery. The buffering capacity of the complex biological medium was found to change throughout the bioconversion. In addition to describing satisfactorily a set of experiments reported in the literature, the model was successfully used to predict metabolite concentrations and the resulting pH in new operating conditions with free pH dynamics. A sensitivity analysis was performed to identify the most influential parameters of the model. The proposed model represents a valuable tool for bioprocess design as it describes the detailed kinetics of 1,3-propanediol oxidation to 3-hydroxypropionic acid by acetic acid bacteria in bioreactor. Additionally, the pH prediction is a major feature of this model, which could guide the identification of optimal operating conditions for microbial activity with a simultaneous in-situ recovery process.

1. Introduction

Biotechnological processes for bulk chemical production have been gaining significant interest over the past decades, as a solution to replace the current chemicals mostly obtained from fossil feedstocks [1]. The production of organic acids through microbial routes is promising in this context as they can be entirely produced from renewable sources. Organic acids present not only a wide range of direct industrial applications but can also be precursors of important bulk and fine chemicals [2]. The demand for a broader bio-based supply of organic acids places this market as one of the main growing markets across bioproducts in the recent years [3].

Among the emerging organic acids, 3-hydroxypropionic acid (3-HP) has gained interest after its classification as one of the most promising bio-based building blocks by the Department of Energy of the United States [4]. Thanks to its two functional groups (carboxyl and β-hydroxyl), 3-HP is a versatile molecule with great potential for further transformation via either chemical or biological processes, or a combination of both, into value-added chemicals, among which acrylic acid is the most noteworthy [4]. Acrylic acid is an important bulk chemical widely used as a precursor of polymers with a total market estimated at 7700 kton in 2021 [5]. It is estimated that the bio-based route could reduce the greenhouse gas emissions related to the production of acrylic acid by at least 81% [6].

In view of this potential, microbial production of 3-HP has improved from metabolic engineering and process engineering standpoints. One of the most promising metabolic pathways identified is the conversion of 1,3-propanediol (1,3-PDO). The bio-based production of 1,3-PDO from renewable resources such as glycerol, and especially glucose, has known major improvements in recent years reaching even the industrial scale. The availability of 1,3-PDO as renewable substrate for bio-transformations is thus expected to increase [7].

An important metabolic pathway for 1,3-PDO conversion into 3-HP has been identified in acetic acid bacteria [8]. These bacteria comprise a set of primary membrane-bound dehydrogenases capable of oxidizing

* Corresponding author.
E-mail address: cristian.trelea@agroparistech.fr (I.-C. Trelea).

https://doi.org/10.1016/j.bej.2024.109346
Received 13 February 2024; Received in revised form 12 April 2024; Accepted 1 May 2024
Available online 4 May 2024

Nomenclature

Abbreviation	Meaning
1,3-PDO	1,3-propanediol
3-HPA	3-hydroxypropionaldehyde
3-HP	3-hydroxypropionic acid
HPLC	High Performance Liquid Chromatography
MAD	Mean absolute deviation
MAE	Mean absolute error
Greek letters	Meaning, Unit
β	Slope of pH inhibition factor, -
κ	Forward reaction kinetic constant, L mol^{-1} h^{-1}
μ	Specific growth rate, h^{-1}
Variable	Meaning, Unit
$[1,3\text{-PDO}]$	Concentration of 1,3-propanediol, mol L^{-1}
[3-HPA]	Concentration of 3-hydroxypropionaldehyde, mol L^{-1}
$[A^-]$	Concentration of 3-HP dissociated species, mol L^{-1}
$[AH]$	Concentration of 3-HP undissociated species, mol L^{-1}
$[AH]_T$	Total 3-HP acid concentration, mol L^{-1}
$[Bu^-]$	Concentration of buffer dissociated species, mol L^{-1}
$[BuH]$	Concentration of buffer undissociated species, mol L^{-1}
$[BuH]_T$	Total buffer concentration, mol L^{-1}
D	Dilution rate, h^{-1}
$f_{pH,\mu}$	pH inhibition factor on growth, -
F	Flow rates, L h^{-1}
$[H^+]$	Proton concentration, mol L^{-1}
K_a	3-HP acid dissociation constant, mol L^{-1}
K_{buff}	Buffer pseudo-species dissociation constant, mol L^{-1}
K_i	Inhibition constant, mol L^{-1}
K_w	Water dissociation constant, mol^2 L^{-2}
n	Inhibition term exponent, -
$[OH^-]$	Hydroxide ion concentration, mol L^{-1}
p	Number of parameters in the model, -
q	Specific production rate, mol_{metab} $mol_{biomass}^{-1}$ h^{-1}
r	Reaction rate, mol L^{-1} h^{-1}
S_i	Main Sobol index related to parameter i, -
S_{T_i}	Total Sobol index related to parameter i, -
t	Time, h
V	Bioreactor volume, L
w_i	Weights attributed in the calibration process, -
$[X]$	Biomass concentration, mol L^{-1}
Y	Yield,mol mol^{-1}

Subscripts/Superscripts

3-HPA	Related to the oxidation of 1,3-propanediol into 3-hydroxypropionaldehyde
a	Related to acid dissociation
AH	Related to the oxidation of 3-hydroxypionaldehyde into 3-hydroxypropionic acid
$buff$	Related to buffer dissociation
$evap$	Related to the evaporation
exp	Experimental data
i	Related to 3-hydroxypropionic acid inhibition
in	Related to the inlet
max	Maximum rate
$samp$	Related to the sampling
sim	Simulated data
S	Related to the substrate
T	Total concentration
w	Related to water dissociation
X	Related to biomass growth

a wide range of alcohols and polyols. In the production of 3-HP, 1,3-PDO is first oxidized into 3-hydroxypropionaldehyde (3-HPA) by a membrane-bound alcohol dehydrogenase and further oxidized into 3-HP by a membrane-bound aldehyde dehydrogenase [9]. This process, known as oxidative fermentation, leads to the accumulation of high amounts of metabolites in the culture broth. The use of acetic acid bacteria to convert 1,3-PDO into 3-HP is advantageous as these microorganisms resist to acidic conditions and high substrate concentrations [10]. Although oxidative fermentation is a well-known process, its implementation for 3-HP production is still challenging due to the inhibition phenomena caused by the acid stress due to a combined effect of 3-HP molecules and pH [11]. There is thus a potential to improve 3-HP production by acetic acid bacteria.

Given the complexity of the phenomena involved, bioprocess design and optimization through fully experimental approaches can be difficult and time-consuming. In contrast, modeling approaches can greatly reduce the experimental effort and be a valuable tool for better understanding, designing and operating bioprocesses. To the best of the authors' knowledge, the only work regarding 3-HP production via 1,3-PDO oxidation using acetic acid bacteria from a modeling standpoint was reported by Li et al. [12]. These authors conducted bioconversions in flasks using immobilized cells of *Acetobacter* sp. CGMCC 8142. They proposed a first-order differential equation to describe 1,3-PDO mass transfer from the medium to the spherical particles containing the cells whereas the kinetics of 3-HP production was described using an empirical function. The main goal of their work was to experimentally optimize the immobilization conditions, while the kinetics of 3-HP production was used as a criterion to compare the performance of different immobilization matrices. A limitation of empirical modeling is that the results are specific to the operating conditions in which they are obtained. Consequently, empirical kinetic modeling provides few insights into limiting mechanisms and can hardly be predictive for new operating conditions.

One of the most important factors to consider in a mathematical model describing organic acid bioproduction is the pH dependence of reaction kinetics. pH strongly affects bacterial metabolism as well as the distribution of acid-base species present in culture media. pH also determines the recovery route, as common downstream processes for organic acid recovery are pH-dependent (e.g. precipitation, reactive liquid-liquid extraction, ion-exchange, nanofiltration, electrodialysis) [13].

During the microbial production of organic acids, the accumulation of acid molecules causes the pH of the medium to decrease. In practical applications, a base is thus constantly added to maintain the pH at a constant setpoint value. Hence, most of mathematical models describing organic acid production are developed considering constant medium pH, neglecting acid-base reactions. Some examples of such models in the literature are proposed for: acetic acid [14], lactic acid [15], and succinic acid [16]. These models are strictly limited to processes conducted at controlled pH, and the prediction of the pH change as a function of the acid concentration is not possible as the acid-base reactions are not included. However, exploring biological acid production without pH control is encouraged due to environmental concerns aiming to limit the use of chemicals. In addition, this operating condition is advantageous for implementing simultaneous in-situ recovery techniques, which are mostly effective at low pH.

A challenge for predicting accurately the pH is the buffering capacity of the medium. Buffering capacity is the resistance to pH changes when an external acid or base is added. Some models have been proposed in the literature to consider the buffering capacity of complex media, especially in lactic acid fermentation [17–19]. These models rely on experimental measurements of pH at different acid concentrations and

can be completely empirical or quasi-mechanistic.

The buffering capacity depends on the composition of the medium, and therefore it is a characteristic that evolves throughout the bioconversion, mainly because of the metabolism of nitrogen sources present in the medium. The studies on the evolution of the buffer capacity of complex media are very limited and have only been reported in fields other than organic acid production, mostly in alcoholic fermentation. The most significant work in terms of modeling was proposed by Akin et al. [20]. The authors proposed a model considering the concentration of multiple acid species measured during the process. In addition, they defined a weak acid pseudo-species called "vinic acid" with the aim of accounting for all the unknown buffering species in the culture medium. Considering these phenomena, the concentration of protons in the medium could be calculated as a function of the composition of the broth at any time.

In the present work, a model of the biological production of 3-HP is proposed based on experimental data from our research group obtained at constant pH [21]. Despite the recognized importance of pH in microbial growth and product formation, existing models fall short in accurately predicting pH changes due to bioconversion processes. Our work addresses this gap by integrating the buffering capacity of the biological medium into the bioconversion modeling. The quasi-mechanistic model proposed by Nicolaï et al. [22] was used to account for the buffer capacity of the complex bioconversion medium. This model presents the advantage of establishing mass balances for dissociated and non-dissociated acid species instead of empirical correlations. The buffering capacity at the beginning and at the end of the bioconversion was considered to account for the observed pH change during the process. The developed model was used to predict the metabolite concentrations using a new operating condition at uncontrolled pH. Operating the process at uncontrolled pH avoids the consumption of alkali for pH control and enhances the performance of separation techniques for subsequent or simultaneous extraction, which are generally favored in acidic conditions (pH $<$ pKa). A sensitivity analysis based on Sobol indices was performed to evaluate the relative importance of the model parameters on the production of 3-HP and to suggest ways to improve the model and the bioconversion process.

2. Material and methods

2.1. Materials

The acetic acid bacterium strain *Acetobacter cerevisiae* CIP 58.66 was purchased as a lyophilizate from the Biological Resource Center of the Pasteur Institute (Paris, France). The lyophilizate was put successively in two liquid cultures: the first containing mannitol and the second containing ethanol. The last culture was aliquoted and stored at -80°C in 1 mL cryotubes with glycerol (20% w/v) as cryoprotectant. Glycerol (CAS number 56–81–5, 97% purity) was purchased from VWR Chemicals (Leuven, Belgium, 99% purity). Yeast extract and Bacto™ peptone were purchased from Organotechnie (La Courneuve, France) and BD-France (Le-Pont-de-Claix, France), respectively. H_2SO_4 (CAS number 7664–93–9, 95% purity) and K_2HPO_4 (CAS number 7758–11–4, 99% purity) were purchased from Sigma-Aldrich (St Louis, USA). 3-hydroxypropionic acid (CAS number 503–66–2, 29.1% w/w in water) and 1,3-propanediol (CAS number 504–63–2, 99.8% purity) were purchased from TCI Europe (Zwijndrecht, Belgium). 3-hydroxypropionaldehyde was obtained through chemical synthesis at URD Agro-Biotechnologies Industrielles (Pomacle-Bazancourt, France) as described by Burgé et al. [23].

2.2. Inoculum preparation

Inoculum was prepared from two successive precultures as described by de Fouchécour et al. [21]. The basal medium for the first culture consisted of 5 g L^{-1} yeast extract, 3 g L^{-1} Bacto™ peptone and 8.71 g L^{-1} K_2HPO_4. Its initial pH was adjusted to 6.5 using 5.5 mol L^{-1} H_2SO_4. After sterilization at 120°C for 20 min, 25 mL was put in a 250 mL baffled shake flask, inoculated with a 1 mL cryotube stock, and incubated for 62 h at 30°C under rotary shaking at 200 rpm. After 62 h, the cultures were found to be in the early stationary phase. For the second culture, 50 mL of the basal medium supplemented with 10 g L^{-1} glycerol was put in a 500 mL baffled shake flask and inoculated using the first culture as a starter to reach an initial cell dry weight of approximately 0.01 g L^{-1}. This second culture was then incubated for 24 h under the same conditions as described above, and later used as a starter for the fed-batch experiments.

2.3. Fed-batch bioconversions in bioreactor

The experiments in the bioreactor started with a growth phase on glycerol. The growth medium contained 5 g L^{-1} yeast extract, 3 g L^{-1} Bacto™ peptone, 8.71 g L^{-1} K_2HPO_4 and 10 g L^{-1} glycerol and its initial pH was adjusted to 5.0 using 5.5 mol L^{-1} H_2SO_4. A volume of 1.2 L of medium was autoclaved in a 3.6 L Labfors 4 bioreactor (Infors HT, Bottmingen, Switzerland). The bioreactor was inoculated at an initial biomass concentration of approximately 0.01 g L^{-1} using the inoculum prepared as described in Section 2.2. In all cultures, temperature was controlled at 30°C, pH evolved freely and pO_2 was controlled at 40% of the saturation value by means of a cascade control loop of stirring speed (100–800 rpm) and air flow (1–4 NL min^{-1}). pH and pO_2 were monitored using a 405-DPAS-SC probe and an InPro 6800 polarographic probe, respectively (Mettler-Toledo, Greifensee, Switzerland).

Once biomass growth reached the early stationary phase (about 32 h), 3-HP production was triggered by a pulse addition of 1,3-PDO to a concentration in the bioreactor of about 0.09 mol L^{-1}. From this point, the strategy of continuous substrate addition differed from the work of de Fouchécour et al. [21]. In the experimental work described by de Fouchécour et al. [21], bioconversions were conducted at controlled pH by the addition of a 6 mol L^{-1} equimolar solution of 1,3-PDO and NH_4OH. The solution was automatically added when the pH of the medium decreased below the set point (pH = 4.0, 4.5 and 5.0), thus, the substrate addition was coupled to pH control. In the present work, the feeding solution composed of 6 mol L^{-1} 1,3-PDO was added at a constant flow rate by a Watson-Marlow 120 U peristaltic pump (Falmouth, UK) and pH was let to evolve freely. In both cases, the feeding solution was filter-sterilized through a filter of 0.22 μm pore diameter before being injected into the bioreactor. All the experiments were performed in duplicate.

2.4. Titration of bioconversion media

Titration curves of total 3-HP concentration versus pH were built by gradually adding known volumes of the commercial solution of 3-HP to the bioconversion broth and monitoring the pH change with a pH-meter pHenomenal 1100 L (VWR, Radnor, PA, USA).

2.5. Analytical techniques

Cell biomass concentration was estimated from an optical density measurement at 600 nm. Optical density was measured using an Evolution 201 spectrophotometer (ThermoScientific, Madison, USA). The relation to cell dry weight (in g L^{-1}) was established using a correlation (Eq. 1) previously determined by de Fouchécour et al. [21]. The correlation was validated for values of optical density ranging from 0 to 0.8. A dilution was prepared, when necessary, to be in the validity range.

$$\textit{Cell dry weight} = 0.59 \times \textit{optical density} \text{ at } 600 \text{ nm} \quad (1)$$

For molar calculations, cell biomass was expressed as equivalent carbon mole assuming the average formula $CH_{1.75}O_{0.5}N_{0.25}$ corresponding to a molecular weight of 25.268 g $Cmol^{-1}$ [24].

Metabolite concentrations were measured by High Performance

Liquid Chromatography (HPLC). The samples containing cells were first centrifuged at 13,000 *g* and 25°C for 10 minutes. The supernatant was then filtered at 0.22 μm and, if necessary, diluted with milliQ ultrapure water before HPLC analysis. The HPLC system was equipped with an Aminex HPX-87 H column (Richmond, CA, USA). For glycerol, 1,3-propanediol and 3-hydroxypropionic acid, the temperature of the column was set at 65°C and the mobile phase used was H_2SO_4 0.5 mmol L^{-1} at a flow rate of 0.4 mL min^{-1}. Regarding 3-hydroxypropionaldehyde, the mobile phase was H_2SO_4 5 mmol L^{-1} circulating at 0.6 mL min^{-1} in the column at 35°C. All the molecules were detected by a refractive index detector (Waters, Guyancourt, France).

3. Modeling

3.1. Model structure

The proposed mathematical model was developed as the combination of two models: a biological model and a buffering capacity model. Each model comprised different parameters estimated using experimental data. A scheme of the whole model is presented in Fig. 1. Section 3.1.1 describe the biological model, and Section 3.1.2 the buffer capacity model, respectively.

3.1.1. Biological model

In the biological model, 1,3-PDO is metabolized for biomass production (*X*), and through the oxidative fermentation pathway producing 3-HPA as an intermediate and 3-HP as the final product. The following assumptions were made:

- The reactor is perfectly mixed: there are no concentration and no temperature gradients.
- There is only one limiting substrate for each biological reaction. All the other substrates (e.g., nitrogen sources, O_2) are in excess.
- The only growth substrate during bioconversion is 1,3-PDO.
- 1,3-PDO and 3-HPA concentrations are below their respective inhibition thresholds.
- All the biomass is active: no cell death was considered and no conversion to an inactive biomass population.
- There is neither substrate nor product loss by evaporation. However, water evaporation was considered.
- There are no side reactions in the oxidative fermentation pathway, i.e., the conversion yields from 1,3-PDO to 3-HPA and from 3-HPA to 3-HP are quantitative.
- 3-HP is produced in its undissociated form.

Mass balances were established for the biomass, 1,3-PDO, 3-HPA and the undissociated species of 3-HP (Eq. (2) – (5)). The biological reaction rates were expressed as modified Monod-like equations considering the inhibitory effect of 3-HP on both growth and oxidative fermentation (Eq. (7) – (9)). The form of the inhibition factor used in this study was previously used by Jiménez-Hornero et al. [25] to describe the inhibitory effect of acetic acid on AAB. Furthermore, an additional inhibition factor was considered in the growth rate (Eq. (7)) due to the inhibitory effect of the pH. The inhibitory effect of pH was only considered on growth as de Fouchécour et al. [21] observed no effect of pH on the specific rates involved in the oxidative fermentation pathway in the studied range. The variation of the volume of the medium due to feed, sampling and evaporation was considered as expressed in Eq. (6). All the equations of the biological model are summarized in Tables 1 and 2.

3.1.2. Buffer capacity model

The buffering capacity model consists of three main acid-base reactions: 3-HP acid dissociation, the dissociation of a buffer pseudo-species and water autoprotolysis. This model was first proposed by Nicolaï et al. [22] to describe the pH in a buffered medium during lactic fermentation. The main assumption of this model is that the buffering capacity of the complex medium can be explained by the presence of 3-HP and a single buffer system composed of the acid pseudo-species *BuH* and its conjugated base Bu^-. To integrate buffering capacity in the biological model, the mass balance of undissociated 3-HP species (Eq. (5)) can be rewritten as expressed in Eq. (11). Eq. (12) – (16) express the mass balances of the other acid-base species considered.

Given that the dissociation rates are significantly faster than the biological rates, the dissociation reactions are considered as almost immediately equilibrated in the medium. Therefore, the dissociation rates were defined as in Eq. (17) – (19) with high backward kinetic constants κ_a, κ_{buff} and κ_w in order for the dissociation reactions to be

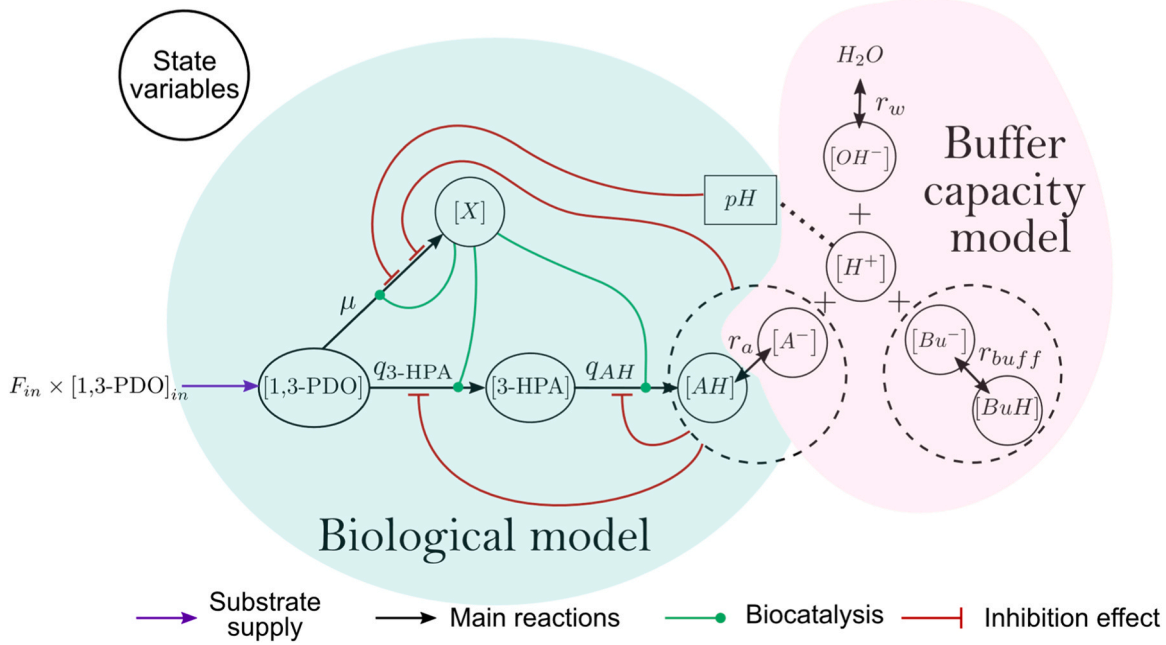

Fig. 1. Schematic representation of the mathematical model of the bioconversion of 1,3-propanediol into 3-HP considering the buffering capacity of the medium.

Table 1
Equations of the biological model.

Mass balances		Eq.
Biomass	$\frac{d[X]}{dt} = \mu[X] - (D_{in} - D_{evap})[X]$	(2)
1,3-PDO	$\frac{d[1,3\text{-PDO}]}{dt} = -\frac{1}{Y_{X/1,3\text{-PDO}}}\mu[X] - q_{3\text{-HPA}}[X] + D_{in}[1,3\text{-PDO}]_{in} - (D_{in} - D_{evap})[1,3\text{-PDO}]$	(3)
3-HPA	$\frac{d[3\text{-HPA}]}{dt} = (q_{3\text{-HPA}} - q_{AH})[X] - (D_{in} - D_{evap})[3\text{-HPA}]$	(4)
Und. 3-HP	$\frac{d[AH]}{dt} = q_{AH}[X] - (D_{in} - D_{evap})[AH]$	(5)
Volume variation		Eq.
	$\frac{dV}{dt} = F_{in} - F_{evap} - F_{samp}$	(6)
Specific biological rates		Eq.
Growth	$\mu = \mu_{max}\frac{[1,3\text{-PDO}]}{K_{S,X} + [1,3\text{-PDO}]}\frac{1}{1 + \left(\frac{[AH]_T}{K_{i,X}}\right)^{n_X}} f_{pH,\mu}; f_{pH,\mu} = \begin{cases} 1 & if\ pH > 5 \\ 1 + \beta(pH - 5) & if 5 - 1/\beta < pH < 5 \\ 0 & if\ pH < 5 - 1/\beta \end{cases}$	(7)
3-HPA production	$q_{3\text{-HPA}} = q_{3\text{-HPA,max}}\frac{[1,3\text{-PDO}]}{K_{S,\ 3\text{-HPA}} + [1,3\text{-PDO}]}\frac{1}{1 + \left(\frac{[AH]_T}{K_{i,3\text{-HPA}}}\right)^{n_{3\text{-HPA}}}}$	(8)
3-HP production	$q_{AH} = q_{AH,max}\frac{[3\text{-HPA}]}{K_{S,AH} + [3\text{-HPA}]}\frac{1}{1 + \left(\frac{[AH]_T}{K_{i,AH}}\right)^{n_{AH}}}$	(9)
Dilution rates		Eq.
	$D_j = \frac{F_j}{V};\ j = \{in, evap, samp\}$	(10)

Table 2
Equations of the buffer capacity model.

Mass balances		Eq.
Und. 3-HP	$\frac{d[AH]}{dt} = q_{AH}[X] - r_a - (D_{in} - D_{evap})[AH]$	(11)
Diss. 3-HP	$\frac{d[A^-]}{dt} = r_a - (D_{in} - D_{evap})[A^-]$	(12)
Und. buffer	$\frac{d[BuH]}{dt} = -r_{buff} - (D_{in} - D_{evap})[BuH]$	(13)
Diss. buffer	$\frac{d[Bu^-]}{dt} = r_{buff} - (D_{in} - D_{evap})[Bu^-]$	(14)
Hydronium ion	$\frac{d[H^+]}{dt} = r_a + r_{buff} + r_w - (D_{in} - D_{evap})[H^+]$	(15)
Hydroxide ion	$\frac{d[OH^-]}{dt} = r_w - (D_{in} - D_{evap})[OH^-]$	(16)
Acid-base dissociation rates		Eq.
3-HP acid dissociation	$r_a = \kappa_a(K_a[AH] - [A^-][H^+])$	(17)
Buffer dissociation	$r_{buff} = \kappa_{buff}(K_{buff}[BuH] - [Bu^-][H^+])$	(18)
Water autoprotolysis	$r_w = \kappa_w(K_w - [OH^-][H^+])$	(19)

equilibrium-limited. The backward constants were thus arbitrarily set to 10^6 L mol^{-1} h^{-1}. In the sensitivity analysis that will be described in Section 4.4, it was verified that the value had negligible impact on the model outputs.

3.2. Parameter estimation

3.2.1. Biological parameters

The proposed biological model required the estimation of 14 parameters listed in Table 3. The parameters were estimated using the experimental data reported by de Fouchécour et al. [21]. Those authors performed bioconversions in duplicate at controlled pH values of 5.0, 4.5 and 4.0, which represents a total of 6 experiments.

Table 3
Parameters of the biological model.

	Growth	**Oxidative fermentation**
Maximum specific rates	μ_{max}	$q_{3\text{-HPA,max}}$, $q_{AH,max}$
Saturation constants	$K_{S,X}$	$K_{S,\ 3\text{-HPA}}$, $K_{S,\ AH}$
Acid inhibition constants and exponents	$K_{i,X}$, n_X	$K_{i,\ 3\text{-HPA}}$, $n_{3\text{-HPA}}$, $K_{i,\ AH}$, n_{AH}
Yield	$Y_{X/1,3\text{-PDO}}$	NA
pH inhibition coefficient	β	NA

Considering the number of parameters, the estimation was divided in four steps, which required to define reduced versions of the model and to use experimental data as inputs. A stepwise approach was adapted in order to increase progressively the number of parameters estimated simultaneously. A major challenge to the estimation of the biological parameters proposed in this work was the lack of good initial guesses to initialize the optimization. Typically, the initial guesses are obtained from the literature. However, so far, no 3-HP production kinetics using acetic acid bacteria have been published.

As a way to find initial guesses, a global optimization algorithm was used. Instead of a unique initial value, a global optimization algorithm starts with a plausible range for each parameter to be estimated. Another advantage of global optimization lies in the thorough exploration of the parameter ranges, avoiding premature convergence to local optima. Unlike local optimization, rather than one estimation, global optimization leads to a set of candidate estimations. Consequently, the best candidate estimation identified through global optimization were good initial guesses to initialize the local optimization approach. More details on the steps of the parameter estimation are available in Supplementary material A.

Considering that the pH control was coupled to the feeding strategy in the experiments of de Fouchécour et al. [21], the feeding flow rate (F_{in}) was interpolated from the experimental volume fed. The sampling and the evaporation flow rates (F_{samp} and F_{evap}, respectively) were also interpolated from the experimental data. The profiles of the different flow rates are presented in Supplementary material C.

The estimation problems were defined to find the parameter values that minimize the cost function expressed in Eq. (20), representing the sum of the weighted squared differences between measured and simulated metabolite concentrations.

$$Cost\ function = \frac{1}{2}\sum_i \sum_{j=1}^{N_i} \left[w_i \left(\frac{y_{i,j}^{exp} - y_{i,j}^{sim}}{\Delta y_i^{exp}} \right) \right]^2 \quad (20)$$

where i represents the species considered ($i = \{1,3\text{-PDO}, 3\text{-HPA}, AH,$

$X\}$), N_i is the number of experimental measurements available for variable i, $y_{i,j}^{exp}$ is the j-th experimental value of variable i, and $y_{i,j}^{sim}$ the corresponding simulated value. Given that each variable i has its own variation range Δy_i^{exp}, they were normalized by dividing by Δy_i^{exp}.

Depending on the choice of the weights (w_i) assigned to the variables in Eq. (20), different sets of estimated parameters can be obtained. Aiming to avoid biased estimations due to a choice of particular weights, a total set of 10^3 weights were randomly sampled from uniform distributions in the interval [1,5] and were used to estimate the parameters. As a result, an observed frequency distribution was obtained for each parameter. The values reported in Section 4.1 correspond to the medians of these distributions.

3.2.2. Buffer capacity parameters

As mentioned in Section 3.1.2, the model of Nicolaï et al. [22] was used to describe the buffering capacity of the medium. This model comprises two parameters to estimate: the buffer dissociation constant K_{buff} and the total buffer concentration $[Bu]_T$. Unlike the biological parameters, the parameters of the buffering capacity model were estimated from titration curves obtained as described in Section 2.4. Considering the main assumptions of the model, the nonlinear equation system presented in Table 4 were solved to find the concentrations at the equilibrium. The pH was thus calculated from the proton concentration in the medium.

3.3. Sensitivity analysis of the model parameters

The global sensitivity of the model parameters was evaluated using the main and the total Sobol indices (S_i and S_{T_i}, respectively), using the estimators proposed by Jansen [27] and Saltelli et al. [28]. The model was simulated 10^4 times, with parameters randomly sampled from normal distributions with the mean equal to the values identified in the parameter estimation process, and standard deviations equal to 10% of the mean values. Regarding the backward dissociation kinetic constants, the parameter values were drawn from uniform distributions in the interval [10^5, 10^7] as these kinetic constants were arbitrarily set to 10^6 L mol^{-1} h^{-1}.

Given that the model proposed in this work is dynamic, the sensitivity indices depend on time. To account for time variation, the main and total Sobol indices were evaluated at $t = \{0.5$ h, 1 h, 5 h, 7.5 h, 10 h, 15 h, 20 h, 25 h, 30 h, 35 h, 40 h, 45 h, 50 h$\}$. The mean indices were then defined as Eqs. (27) and (28).

$$S_i^* = \frac{1}{t_f - t_0}\int_{t_0}^{t_f} S_i(t)dt \tag{27}$$

$$S_{T_i}^* = \frac{1}{t_f - t_0}\int_{t_0}^{t_f} S_{T_i}(t)dt \tag{28}$$

3.4. Numerical methods

All the numerical methods were implemented in MATLAB R2022b (The MathWorks Inc., Natick, MA) including the Statistics and Optimization toolboxes. The systems of ordinary differential equations were solved using the *ode15s* function, which is a variable-order method for the solution of stiff problems.

During the estimation of the parameters of the biological model, the global optimization approach was undertaken using the genetic algorithm NSGA-II implemented in MATLAB by Song [29], considering intermediate crossover and gaussian mutation. Based on preliminary tests, the number of individuals was set to 100 and the number of generations was 50. Local optimization problems were solved using the *lsqnonlin* function implementing the 'Trust-region-reflective' algorithm [30]. A non-negative constraint was defined to prevent the parameters from taking negative values.

The function *fsolve* implementing the "trust-region" method [30] was used for solving the non-linear equation system related to buffering capacity presented in Table 4. The parameters of this model were estimated using the *nlinfit* function.

Table 4
Nonlinear equation system used to describe titration curves.

*Acid dissociation**	$K_a = \frac{[A^-][H^+]}{[AH]}$	(21)
Buffer dissociation	$K_{buff} = \frac{[Bu^-][H^+]}{[BuH]}$	(22)
Water dissociation	$K_w = [OH^-][H^+]$	(23)
*Mass balance acid species***	$[AH]_T = [AH] + [A^-]$	(24)
Mass balance buffer pseudo species	$2\,[Bu]_T = [BuH] + [Bu^-]$	(25)
Charge balance	$[A^-] + [OH^-] + [Bu^-] = [H^+] + [Bu]_T$	(26)

*K_a was taken from [26].
**$[AH]_T$ were known from the controlled additions in the titration experiment.

4. Results and discussion

4.1. Biological model

The estimated parameters using the stepwise approach are presented in Table 5. The median absolute deviation (MAD) of each parameter is also reported as a means of measuring the dispersion of the observed frequency distributions.

All the parameters related to the growth were estimated with MAD values lower than 10% compared to their median, except for $Y_{X/1,3\text{-PDO}}$, whose MAD/median is equal to 11.3%. The parameters related to the oxidative fermentation were estimated with MAD to median ratios ranging mainly from 8% to 30%. The parameters $q_{3\text{-HPA}}$ and $K_{S,3\text{-HPA}}$, related to the oxidation of 1,3-PDO into 3-HPA were estimated with MAD values equal to 50% of their median values. High MAD values could be an indication of poor practical identifiability of both parameters. Indeed, if in Eq. (8), 1,3-PDO concentration is much less than $K_{S,3\text{-HPA}}$, the product between the specific production rate and the Monod-like factor can be simplified to the ratio $q_{3\text{-HPA},max}/K_{S,3\text{-HPA}}$ multiplied by the concentration of 1,3-PDO as shown in Eq. (29). Consequently, $q_{3\text{-HPA},max}$ and $K_{S,3\text{-HPA}}$ cannot be determined separately but their ratio can be identified with a reasonable uncertainty (MAD/

Table 5
Estimated parameters of the biological model.

Parameter	Median	MAD	MAD/median (%)	Units
Growth				
μ_{max}	1.06	0.05	4.7%	h^{-1}
$K_{S,X}$	0.33	0.02	6.1%	mol L^{-1}
$K_{i,X}$	0.128	0.006	4.7%	mol L^{-1}
n_X	3.54	0.01	0.3%	-
$Y_{X/1,3\text{-PDO}}$	0.80	0.09	11.3%	mol$_X$ mol$_{1,3\text{-PDO}}^{-1}$
β*	0.375	—	—	-
Oxidative fermentation				
$q_{3\text{-HPA,max}}$	4	2	50.0%	mol$_{3\text{-HPA}}$ mol$_X^{-1}$ h^{-1}
$q_{AH,max}$	17	4	23.5%	mol$_{AH}$ mol$_X^{-1}$ h^{-1}
$K_{S,3\text{-HPA}}$	0.4	0.2	50.0%	mol L^{-1}
$K_{S,AH}$	0.05	0.01	16.7%	mol L^{-1}
$K_{i,3\text{-HPA}}$	0.72	0.06	8.3%	mol L^{-1}
$K_{i,AH}$	0.5	0.1	20.0%	mol L^{-1}
$n_{3\text{-HPA}}$	3.2	0.9	25.0%	-
n_{AH}	1.8	0.5	27.8%	-
$q_{3\text{-HPA,max}}/K_{S,3\text{-HPA}}$	13	2	15.4%	L mol^{-1} h^{-1}
$\mu_{max}/K_{S,X}$	3.1	0.3	9.7%	L mol^{-1} h^{-1}
$q_{AH,max}/K_{S,AH}$	379	31	8.2%	L mol^{-1} h^{-1}

* β was calculated from the experimental maximum growth rate as a function of pH (described in Supplementary material C).

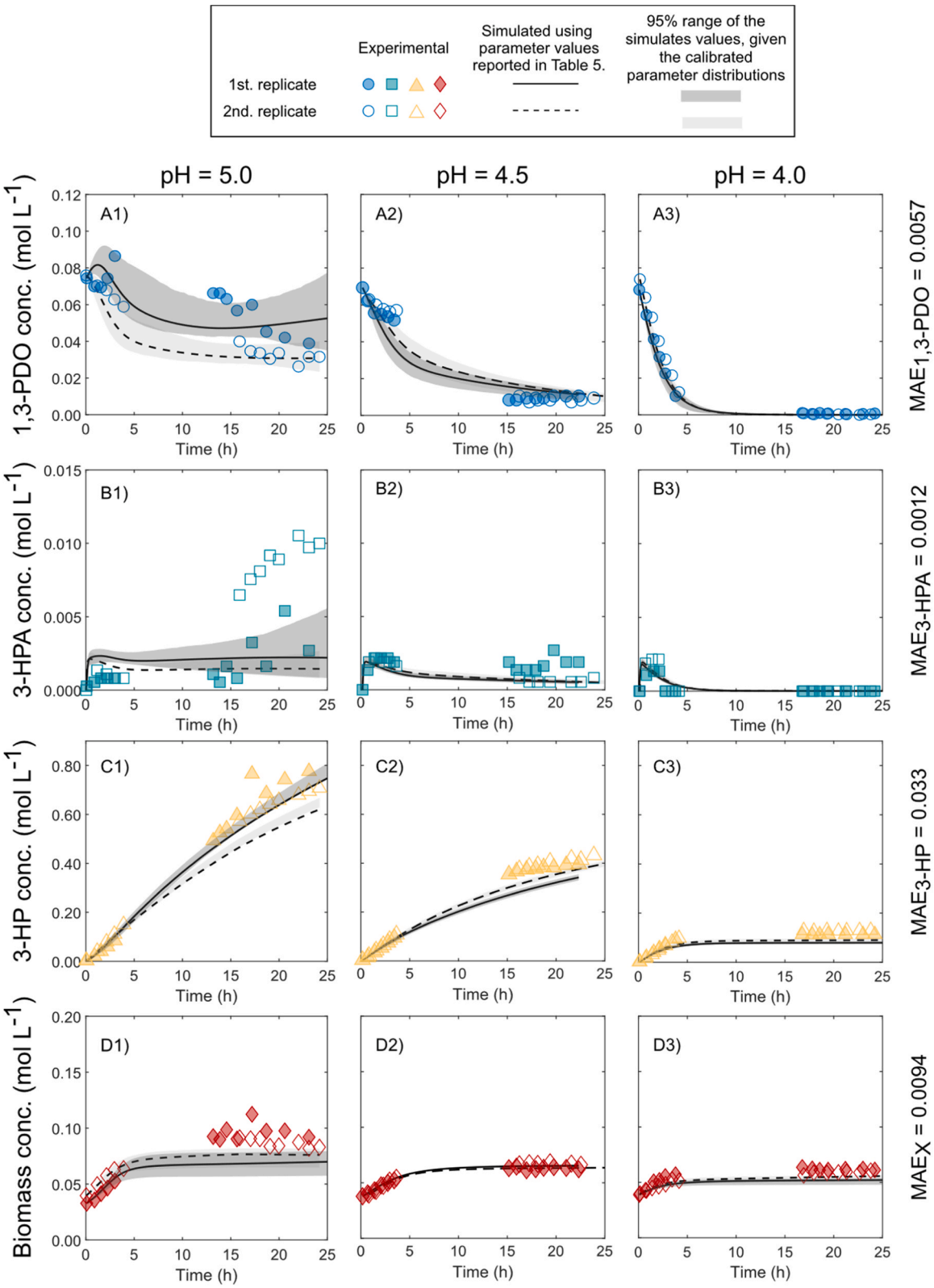

Fig. 2. Results of the model simulations with the determined biological parameters. Experimental data by de Fouchécour et al. [21] used for model calibration.

median = 15.4%, Table 5).

If

$$[1,3\text{-PDO}] \ll K_{S,3\text{-HPA}}:$$

$$q_{3\text{-HPA},max}\frac{[1,3\text{-PDO}]}{K_{S,\ 3\text{-HPA}}+[1,3\text{-PDO}]} \approx \frac{q_{3\text{-HPA},max}}{K_{S,3\text{-HPA}}}[1,3\text{-PDO}] \quad (29)$$

The lack of identifiability of parameters in Monod-like expressions has been widely studied in the literature (ex. in [31]). One of the main difficulties is related to the high correlation between the maximum rate and the substrate saturation constant. In this case, both parameters $q_{3\text{-HPA},max}$ and $K_{S,3\text{-HPA}}$ were indeed found to be highly correlated (0.993 according to the correlation matrix presented in Supplementary material D., Table D.1).

The other couples of parameters related to Monod-like expressions (μ_{max} and $K_{S,X}$ for growth; and $q_{AH,max}$ and $K_{S,AH}$ for 3-HPA oxidation) were also found to be highly correlated (Supplementary material D., Table D.1), nevertheless unlike $q_{3\text{-HPA},max}$ and $K_{S,3\text{-HPA}}$, the dispersions of the observed frequency distributions were lower (MAD/median ratio < 24%, Table 5).

As previously discussed, the estimation of the 'true' values of the parameters in modeling biological systems can be challenging, or even impossible depending on the data available. Nevertheless, the goal of building a mathematical model is also to make predictions despite the lack of identifiability of some parameters. Jiménez-Hornero et al. [25] illustrated this point in the study of acetic acid production from ethanol using acetic acid bacteria cultivated in fed-batch mode in bioreactor.

The simulations obtained with the parameters reported in Table 5 are presented in Fig. 2. Despite the simplifying assumptions, the model successfully described the main phenomena observed for all the considered species and at all the pH values tested. In both experiments at pH = 5.0, the behavior of 1,3-PDO concentrations, characterized by substrate consumption slowing down during the experiment, were well described by the model (Fig. 2.A1). Furthermore, the model successfully reproduced the slight 1,3-PDO accumulation of substrate observed at the beginning of one of the replicates (filled circles). At pH = 4.5 and pH = 4.0, the strictly decreasing behavior of both replicates was well simulated (Fig. 2. A2 and A3). The mean absolute error (MAE) in the prediction of 1,3-PDO was equal to 0.0057 mol L^{-1}, which corresponds to approximately 6% of 1,3-PDO variation range (0 – 0.09 mol L^{-1}).

The peak reached by 3-HPA concentrations during the first hours of bioconversion was well predicted by the model (Fig. 2.B1, B2 and B3). The accumulation of 3-HPA observed at pH = 5.0 after 15 h was not reproduced by the model. The MAE in the prediction of 3-HPA concentrations was equal to 0.0012 mol L^{-1} while the concentrations ranged in most cases from 0 to 0.005 mol L^{-1}, corresponding to around 24% of the variation range.

The model successfully simulated the concentration of 3-HP accumulated in the broth in the three pH conditions (Fig. 2.C1, C2 and C3). The MAE in the acid concentration was equal to 0.033 mol L^{-1} representing around 4% of its variation range (0 – 0.8 mol L^{-1}). The biomass concentration was also well simulated (Fig. 2.D1, D2 and D3), with a MAE representing around 16% of the biomass variation range observed.

It also appears in Fig. 2 that in spite of the parametric uncertainty (Table 5), the uncertainty on the model predictions was quite limited (grey areas in Fig. 2). This is particularly true for the most important model output, the produced 3-HP concentration (Fig. 2.C1, C2 and C3).

4.2. Buffer capacity of the medium

The titration curve obtained using the medium at the beginning of the bioconversion is illustrated in Fig. 3 as a semi-log plot (circles). The pH showed a decreasing behavior with a concavity change. For the sake of comparison, if the pH of an unbuffered medium is estimated using Eq. (21) and (24), it shows a linear decreasing trend (dashed line).

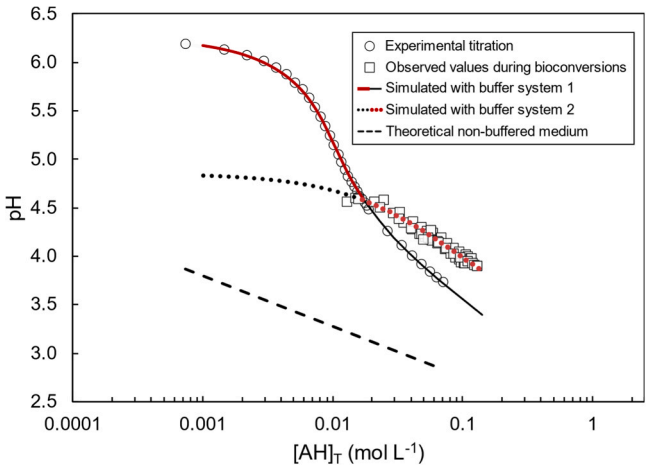

Fig. 3. pH as a function of total 3-HP concentrations. Red curves represent the final model used for predicting the pH.

The pH in the complex medium used in this study differs from that of an unbuffered medium by up to 2.5 pH units at 3-HP concentrations lower than 0.01 mol L^{-1}, and up to 1.5 pH units at 3-HP concentrations higher than 0.01 mol L^{-1}. Thus, the buffering capacity in the medium must be considered as pH is essential for both biological phenomena and subsequent acid extraction techniques.

The pH values measured during the bioconversions as a function of the 3-HP concentration measured by HPLC (squares: data by de Fouchécour et al. [21]) showed a deviation from the experimental titration curve of the initial medium for total acid concentrations higher than 0.017 mol L^{-1}. This is likely linked to an evolution of the buffering capacity of the medium during the bioconversion experiments. The experimental titration data were used to estimate the parameters of a first buffer system (buffer 1) as described in Section 3.2.2. The resulting simulated data are presented in Fig. 3 (solid line). The parameters of a second buffer system (buffer 2) were estimated using the data obtained during the bioconversions reported by de Fouchécour et al. [21]. The simulated results are also presented in Fig. 3 (dotted line). The parameters determined for buffer systems 1 and 2 are presented in Table 6. In both cases, the parameters were estimated with good accuracy (coefficient of variation < 5%).

In order to consider the evolution of buffering capacity over time, the buffer system 1 was considered as representative of the buffering capacity of the medium at early stages of the bioconversion (when total 3-HP concentration was lower than 0.017 mol L^{-1}). The buffer system 2 was considered as representative of the buffering capacity of the medium at later stages (when total 3-HP concentration was higher than 0.017 mol L^{-1}). The final buffering capacity model consisted in switching from buffer 1 to buffer 2 once total 3-HP reached the intersection point at 0.017 mol L^{-1}. This model is represented in bold lines in Fig. 3.

4.3. Model validation using a new operating condition: uncontrolled pH

As described in the previous sections, the model proposed in Section

Table 6
Parameter values for the buffer capacity model.

Parameter *	Buffer 1 For $[AH]_T$ < 0.017 mol L^{-1}	Buffer 2 For $[AH]_T$ > 0.017 mol L^{-1}	Unit
pK_{buff}	6.275 ± 0.004	4.852 ± 0.003	–
$[Bu]_T$	$9.7 \times 10^{-3} \pm 0.2 \times 10^{-3}$	$3.2 \times 10^{-2} \pm 0.1 \times 10^{-2}$	mol L^{-1}

* reported as value ± standard error

3.1.1 successfully simulated the evolution of the different species in bioconversion experiments at constant pH using the feeding, sampling and evaporation profiles as inputs. After including the buffering capacity model (equations presented in Section 3.1.2 and parameter estimation in Section 3.2.2), the model was validated using experimental data obtained by conducting fed-batch bioconversions with constant continuous substrate supply and free pH (i.e., no pH control). Two independent replicates were performed to this purpose.

In order to select the feeding flowrate, several substrate supply conditions were explored in simulation by varying the feeding flow rate in the range $0.74 \times 10^{-3} - 4.4 \times 10^{-3}$ L h^{-1}. A feeding flow rate of 0.87×10^{-3} L h^{-1} was selected for experimental validation as it was the highest feeding rate allowing 1,3-PDO concentration to be maintained at a stationary low value (0.003 mol L^{-1}) while producing 3-HP at a constant rate, according to the model. The results of two replicate experiments and model predictions are presented in Fig. 4.

Experimentally, the initial 1,3-PDO pulse injected to trigger the bioconversion was depleted in approximately 4 h (Fig. 4.A). This rapid consumption produced a quick accumulation of 3-HP in the broth (Fig. 4.B), with a transient accumulation of 3-HPA as intermediate (Fig. 4.D). In parallel, biomass showed a negligible growth phase (Fig. 4.C) and the pH of the medium decreased from 6.2 to about 3.7 (Fig. 4.E). After 12 h of bioconversion, the concentration of 1,3-PDO increased steadily until the end of the experiments indicating that the rate of addition was greater than the rate of consumption. The mass balances throughout the bioconversions are presented in Fig. 5.

The new condition tested in these experiments showed a maximum 3-HP titer of approximately 0.27 mol L^{-1} and an average productivity of 0.005 mol L^{-1} h^{-1}. This titer means a 2.4-fold increase over that obtained at pH = 4.0 by de Fouchécour et al. [21]. However, the average productivity decreased by almost 30%. The advantage of performing bioconversions at free pH is that no base is consumed for pH control and

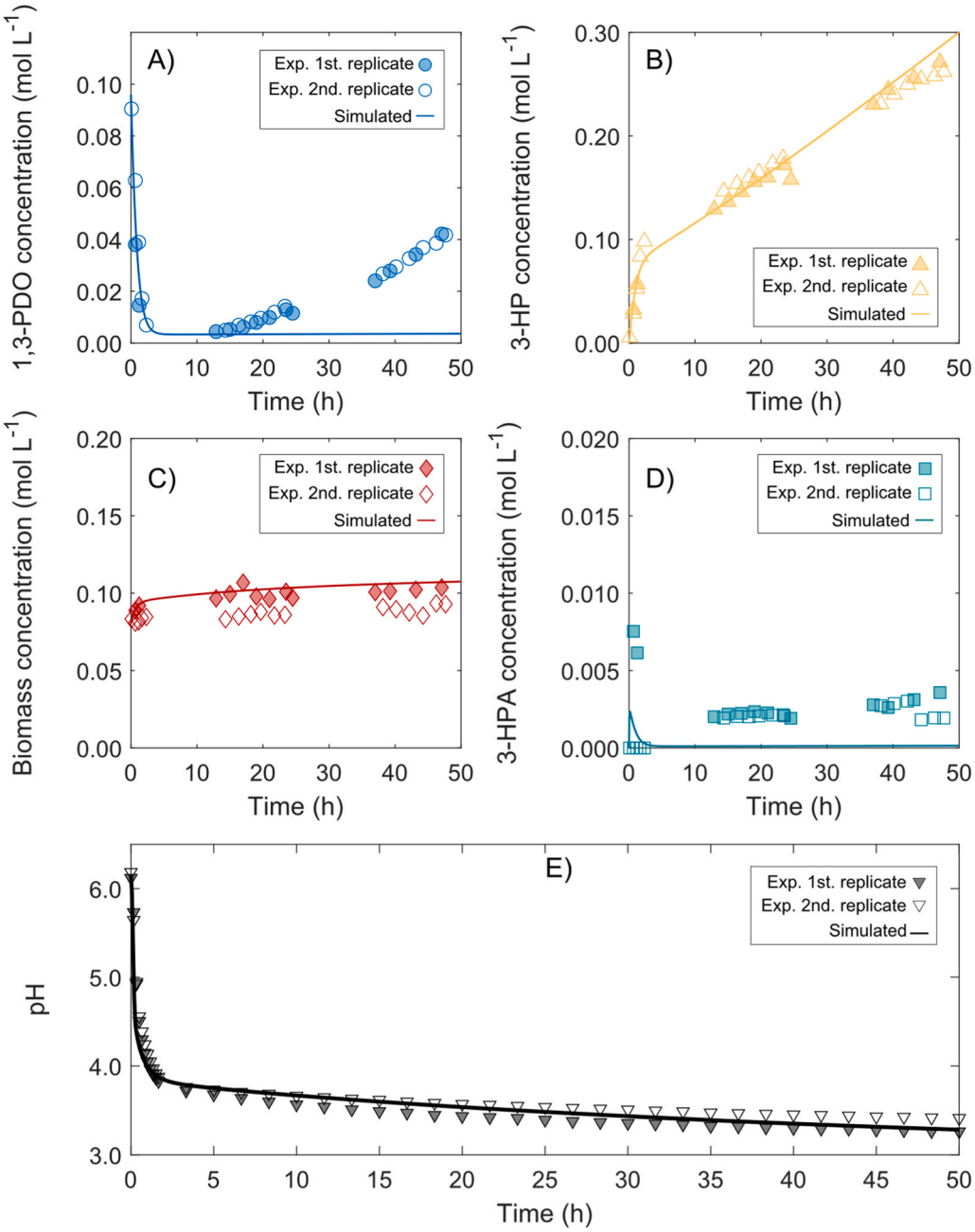

Fig. 4. Experimental validation of the model at the new operating condition.

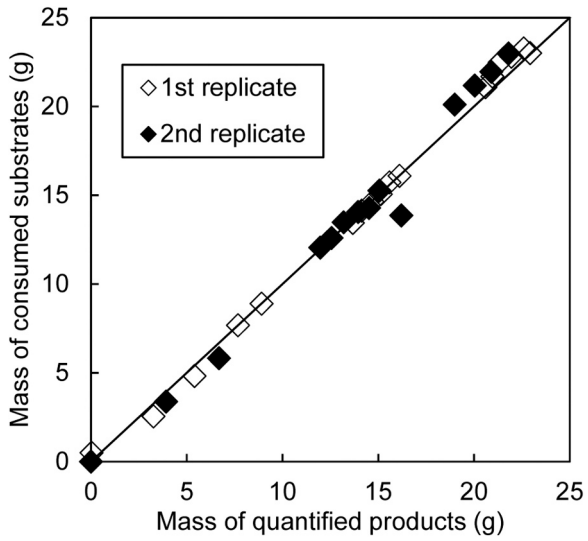

Fig. 5. Mass balances throughout the bioconversions at uncontrolled pH.

Table 7
Mean absolute prediction errors (MAE) for the validation experiments.

Variable	MAE	Variation range
1,3-PDO concentration (mol L^{-1})	0.014	0.004–0.091
3-HPA concentration (mol L^{-1})	0.002	0.0–0.008
3-HP concentration (mol L^{-1})	0.013	0.0–0.27
Biomass concentration (mol L^{-1})	0.010	0.081–0.11
pH (-)	0.072	3.26–6.19

that downstream extraction could be favored by the low pH of the medium.

In the simulation results, most of the trends were correctly predicted by the model. The mean absolute errors (MAE) of the predictions are reported in Table 7. Regarding the concentration of 1,3-PDO, the initial decrease observed in the first 4 h was well predicted but not the accumulation of 1,3-PDO after 12 h. In terms of prediction performance, the MAE in the prediction of 1,3-PDO was equal to 0.014 mol L^{-1}, which represents 16% of the 1,3-PDO variation range during the experiments. As one might expect, the model was less accurate in the new conditions than it was in the calibration experiments.

After the first 4 h of bioconversion, the 1,3-PDO oxidation rate decreased despite the constant substrate supply. This phenomenon is likely related to an inhibitory effect of low pH values on the oxidative fermentation. Even if de Fouchécour et al. [21] observed no effect in the pH range 4.0 – 5.0, in the validation experiment the pH decreased well below 4.0 (Fig. 4.E). Performing bioconversions at lower pH would allow to quantify its effect on the metabolic pathway yielding 3-HP and further improve the model.

The model predicted satisfactorily the accumulation of 3-HP throughout the experiments (Fig. 4.B), including the initial rapid increase as well as the constant production rate observed afterwards. The MAE in the prediction of 3-HP concentration represented 5% of its variation range, which is similar to the calibration experiments. The slight gap observed after 40 h of bioconversion (~ 0.01 mol L^{-1}) could be linked to the decrease of 1,3-PDO oxidation rate previously mentioned.

The model predicted a limited biomass growth considering pH and 3-HP inhibition (Fig. 4.C). For biomass concentration, the model performed with less accuracy than in the calibration experiments (MAE representing 34% of the variation range). This could be expected as the pH inhibition was extrapolated from the results observed in the literature in the range 4.0 – 5.0.

The initial accumulation of 3-HPA was underestimated and a gap of approximately 0.002 mol L^{-1} was observed between the experimental value attained after the transient accumulation and the predicted value (Fig. 4.D). The MAE to the variation range ratio was equal to 25%, which is comparable to that observed in the calibration experiments.

Regarding pH, the predicted values were mostly comprised between the observed experimental values presented in Fig. 4.E for the two replicate experiments. The model had a MAE of 0.072 pH units, which represents 2% of the observed pH variation range. Therefore, the strategy of shifting between two different buffer systems was effective to accurately predict the pH of the medium. The inclusion of buffering capacity and its change over time is a major feature of the proposed model describing organic acid production.

4.4. Sensitivity analysis of estimated model parameters

The Sobol indices represent the fraction of the variance of the output explained by a given model parameter. The main Sobol indices correspond to the effect of a single parameter while the total indices include the main effect as well as the interaction of that parameter with the others. The Sobol indices were used for evaluating the influence of the estimated parameters of the biological model and the buffering capacity model on the most important input of the model: the total 3-HP concentration. The operating conditions corresponded to that identified in the previous section, i.e., constant substrate feeding rate and uncontrolled pH. The 13 parameters of the biological model, and the 7 parameters of the buffering capacity model were included in the sampling process described in Section 3.3. The average main and total indices over time were calculated and sorted in descending order. Only the parameters that showed main and total Sobol indices higher than 0.05 were considered as influential and are presented in Fig. 6. As the main Sobol indices were identical to the total indices, only the main indices are presented. The similarity between the main and total indices suggests that the effect of each parameter was almost linear and no interaction was observed between the parameters in the studied sampling range.

The dissociation constant of the first buffer system (pKa_{buff1}) was found to be the most influential parameter. This parameter was found to be essential to accurately describe the pH of the medium, which influences the microbial growth, which in turn governs all bioconversion reactions. The importance of this parameter highlights the importance of considering the buffer capacity of the medium. In practice, the buffering

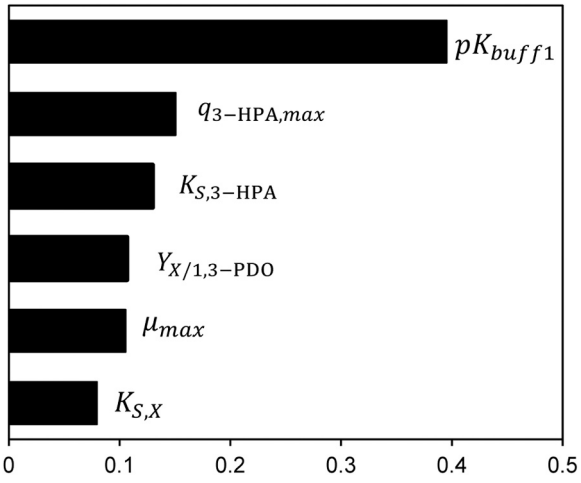

Fig. 6. Time-averaged main Sobol indices of the most influential parameters, considering total 3-HP concentration as model output.

capacity attenuates the pH decrease caused by the accumulation of acid molecules. It could be used as a criterion to determine the amount of substrate and feeding rate that could be supplied without decreasing the medium pH to inhibitory levels due to 3-HP production.

Some of the influential parameters are related to 1,3-PDO oxidation into 3-HPA, namely the maximum 3-HPA production rate ($q_{3\text{-HPA},max}$) and the substrate saturation constant ($K_{S,3\text{-HPA}}$). Despite the relatively high uncertainty described before, the ratio between both parameters was correctly estimated, which was important to make predictions using the model as discussed in Section 4.1. Considering that 3-HPA is an intermediate, the production rate of 3-HPA could be the rate-limiting step in the operating conditions used in the model validation (Section 2.3). The feeding rate of 1,3-PDO could thus be increased aiming to increase the 3-HPA production rate. However, the maximum 1,3-PDO feeding rate must be carefully chosen to avoid both 1,3-PDO and 3-HPA from accumulating in the medium above inhibitory levels.

It was expected that some parameters related to the biomass growth would be found influential considering that biomass concentration is directly linked to all the biological rates. In this case, the influential parameters are the growth yield on 1,3-PDO ($Y_{X/1,3\text{-PDO}}$), the maximum growth rate (μ_{max}) and the growth substrate saturation constant ($K_{S,X}$). As mentioned in Section 4.3, the observed growth phase on 1,3-PDO was very limited. The high sensitivity of the biomass-related parameters suggests the possibility to improve the process by optimizing the previous culture steps in order to increase the cell density before starting the 1,3-PDO feeding phase.

The kinetic constants describing the acid-base reactions mentioned in Section 3.1.2 were found to have no effect on the output in the defined parameter space, confirming the assumption of quasi-equilibrium for these reactions.

5. Conclusion

The bioconversion of 1,3-propanediol into 3-hydroxypropionic acid using acetic acid bacteria was studied. A mathematical model of the bioconversion was built considering acid-base reactions in addition to biological reactions to predict the concentrations of the main species involved in the process as well as the pH of the medium. The biological parameters of the model were estimated using experimental bioconversion data obtained by de Fouchécour et al. [21] at constant pH. The buffering capacity of the complex broth used in this work was described using the model proposed by Nicolaï et al. [22]. In order to take into account the change of the broth composition over time, a shift between two different buffer systems was introduced. Buffering capacity and its time change is rarely considered in models describing the microbial production of organic acids. The developed model correctly predicted metabolite profiles and pH in a new set of fed-batch experiments performed at uncontrolled pH. Therefore, the proposed model is a valuable tool for bioprocess design as production kinetics can be explored using different operating conditions, especially those implying pH variations. Considering these features, this work is a key ingredient in the development of an integrated production-extraction model as both biological production and in-situ extraction processes strongly depend on pH. An integrated model will allow the selection of optimal conditions conciliating the bioconversion and the extraction rates, which are often contradictory, especially with respect to pH. Since acetic acid bacteria are able to produce different acids from their respective alcohols with similar metabolic pathways [32], the presented strategy could be adapted for the production and in-situ extraction of multiple organic acids.

CRediT authorship contribution statement

Ioan-Cristian Trelea: Writing – review & editing, Supervision, Software, Methodology, Formal analysis, Conceptualization. **Claire Saulou-Bérion:** Writing – review & editing, Supervision, Methodology, Conceptualization. **Violaine Athès:** Writing – review & editing, Supervision, Methodology, Conceptualization. **Marwen Moussa:** Writing – review & editing, Supervision, Methodology, Conceptualization. **Henry-Eric Spinnler:** Writing – review & editing, Supervision, Methodology, Conceptualization. **Kevin Lachin:** Writing – review & editing, Methodology, Conceptualization. **Florence de Fouchécour:** Writing – review & editing, Visualization, Validation, Software, Investigation, Formal analysis, Conceptualization. **Pedro Arana-Agudelo:** Writing – original draft, Visualization, Validation, Software, Methodology, Investigation, Formal analysis, Conceptualization.

Declaration of Competing Interest

The authors declare that they have no known competing financial interests or personal relationships that could have appeared to influence the work reported in this paper.

Data Availability

Data will be made available on request.

Acknowledgments

Pedro Arana-Agudelo and Florence de Fouchécour doctoral grants were awarded from the ABIES doctoral school of Université Paris-Saclay. The authors would like to acknowledge URD ABI (Reims, France) for the synthesis of 3-HPA for HPLC standards.

Appendix A. Supporting information

Supplementary data associated with this article can be found in the online version at doi:10.1016/j.bej.2024.109346.

References

[1] J. Spekreijse, K. Vikla, M. Vis, K. Boysen-Urban, G. Philippidis, R. M'barek, Bio-based Value Chains For Chemicals, Plastics and Pharmaceuticals, EUR 30653 EN, Luxembourg, Publication Office of the European Union, 2021, https://doi.org/10.2760/712499.

[2] S. Alonso, M. Rendueles, M. Díaz, Microbial production of specialty organic acids from renewable and waste materials, Crit. Rev. Biotechnol. 35 (2015) 497–513, https://doi.org/10.3109/07388551.2014.904269.

[3] E. de Jong, H. Stichnothe, G. Bell, H. Jørgensen, Bio-based chemicals: a 2020 update, 2020, IEA Bioenergy, 2020. ⟨https://www.ieabioenergy.com/wp-content/uploads/2020/02/Bio-based-chemicals-a-2020-update-final-200213.pdf⟩ (accessed 13 February 2024).

[4] J.J. Bozell, G.R. Petersen, Cutting-edge research for a greener sustainable future Technology development for the production of biobased products from biorefinery carbohydrates - the US Department of Energy's "Top 10" revisited, Green. Chem. 12 (2010), https://doi.org/10.1039/B922014C.

[5] Statista, Mark. Vol. acrylic Acid. Worldw. 2015 2021, Forecast 2022 2029 (2023). ⟨https://www.statista.com/statistics/1245262/acrylic-acid-market-volume-worldwide/⟩ (accessed 13 March 2023).

[6] K. Huang, X. Peng, L. Kong, W. Wu, Y. Chen, C.T. Maravelias, Greenhouse gas emission mitigation potential of chemicals produced from biomass, ACS Sustain. Chem. Eng. 9 (2021) 14480–14487, https://doi.org/10.1021/acssuschemeng.1c04836.

[7] R. Gérardy, D.P. Debecker, J. Estager, P. Luis, J.C.M. Monbaliu, Continuous flow upgrading of selected C2-C6 platform chemicals derived from biomass, Chem. Rev. 120 (2020) 7219–7347, https://doi.org/10.1021/acs.chemrev.9b00846.

[8] P. Zhao, P. Tian, Biosynthesis pathways and strategies for improving 3-hydroxypropionic acid production in bacteria, World J. Microbiol. Biotechnol. 37 (2021), https://doi.org/10.1007/s11274-021-03091-6.

[9] J. Zhu, J. Xie, L. Wei, J. Lin, L. Zhao, D. Wei, Identification of the enzymes responsible for 3-hydroxypropionic acid formation and their use in improving 3-hydroxypropionic acid production in *Gluconobacter oxydans* DSM 2003, Bioresour. Technol. 265 (2018) 328–333, https://doi.org/10.1016/j.biortech.2018.06.001.

[10] X. Qiu, Y. Zhang, H. Hong, Classification of acetic acid bacteria and their acid resistant mechanism, AMB Express 11 (2021), https://doi.org/10.1186/s13568-021-01189-6.

[11] A. Vidra, Á. Németh, Bio-based 3-hydroxypropionic acid: a review, Period. Polytech. Chem. Eng. 62 (2018) 156–166, https://doi.org/10.3311/PPch.10861.

[12] J. Li, H. Zong, B. Zhuge, X. Lu, H. Fang, J. Sun, Immobilization of *Acetobacter* sp. CGMCC 8142 for efficient biocatalysis of 1, 3-propanediol to 3-hydroxypropionic

acid, Biotechnol. Bioprocess Eng. 21 (2016) 523–530, https://doi.org/10.1007/s12257-016-0022-y.
[13] C. Béal, P. Arana-Agudelo, T. Farel, M. Moussa, V. Athès, Lactic acid microbial production and recovery: Review and recent advances in bioprocess integration, in: D. Montet, R.C. Ray, V.A. De Carvalho Azevedo, S. Paramithiotis (Eds.), Lact. Acid Bact. as Cell Factories, 1st ed., Woodhead Publishing, 2023, pp. 77–108, https://doi.org/10.1016/B978-0-323-91930-2.00016-X.
[14] J.E. Jiménez-Hornero, I.M. Santos-Dueñas, I. García-García, Optimization of biotechnological processes. The acetic acid fermentation. Part I: the proposed model, Biochem. Eng. J. 45 (2009) 1–6, https://doi.org/10.1016/j.bej.2009.01.009.
[15] A.W. Schepers, J. Thibault, C. Lacroix, *Lactobacillus helveticus* growth and lactic acid production during pH controlled batch cultures in whey permeate yeast extract medium. Part II kinetic modeling and model validation, Enzym. Microb. Technol. 30 (2002) 187–194.
[16] I.A. Escanciano, M. Ladero, Á. Blanco, V.E. Santos, Succinic acid production by *Actinobacillus succinogenes* using acid and enzymatic hydrolysates of potato and beer wastes and repeated batch operation, Biomass. Bioenergy 181 (2024), https://doi.org/10.1016/j.biombioe.2023.107034.
[17] K.M. Vereecken, J.F. Van Impe, Analysis and practical implementation of a model for combined growth and metabolite production of lactic acid bacteria, Int. J. Food Microbiol. 73 (2002) 239–250, https://doi.org/10.1016/S0168-1605(01)00641-9.
[18] F. Leroy, L. De Vyust, A combined model to predict the functionality of the bacteriocin-producing *Lactobacillus sakei* strain CTC 494, Appl. Environ. Microbiol. 69 (2003) 1093–1099, https://doi.org/10.1128/AEM.69.2.1093.
[19] D. Charalampopoulos, J.A. Vázquez, S.S. Pandiella, Modelling and validation of *Lactobacillus plantarum* fermentations in cereal-based media with different sugar concentrations and buffering capacities, Biochem. Eng. J. 44 (2009) 96–105, https://doi.org/10.1016/j.bej.2008.11.004.
[20] H. Akin, C. Brandam, X.M. Meyer, P. Strehaiano, A model for pH determination during alcoholic fermentation of a grape must by *Saccharomyces cerevisiae*, Chem. Eng. Process. Process. Intensif. 47 (2008) 1986–1993, https://doi.org/10.1016/j.cep.2007.11.014.
[21] F. de Fouchécour, A. Lemarchand, H.É. Spinnler, C. Saulou-Bérion, Efficient 3-hydroxypropionic acid production by *Acetobacter* sp. CIP 58.66 through a feeding strategy based on pH control, AMB Express 11 (2021), https://doi.org/10.1186/s13568-021-01291-9.
[22] B.M. Nicolaï, J.F. Van Impe, B. Verlinden, T. Martens, J. Vandewalle, J. De Baerdemaeker, Predictive modelling of surface growth of lactic acid bacteria in vacuum-packed meat, Food Microbiol. 10 (1993) 229–238, https://doi.org/10.1006/fmic.1993.1025.
[23] G. Burgé, A.L. Flourat, B. Pollet, H.E. Spinnler, F. Allais, 3-hydroxypropionaldehyde (3-HPA) quantification by HPLC using a synthetic acrolein-free 3-hydroxypropionaldehyde system as analytical standard, RSC Adv. 5 (2015) 92619–92627, https://doi.org/10.1039/c5ra18274c.
[24] D. Herbert, P.J. Phipps, R.E. Strange, Chemical analysis of microbial cells. Methods Microbiol, Elsevier, 1971, pp. 209–344.
[25] J.E. Jiménez-Hornero, I.M. Santos-Dueñas, I. García-García, Optimization of biotechnological processes. The acetic acid fermentation. Part II: Practical identifiability analysis and parameter estimation, Biochem. Eng. J. 45 (2009) 7–21, https://doi.org/10.1016/j.bej.2009.01.010.
[26] D.R. Lide, ed., CRC Handbook of chemistry and physics (internet version), 96th ed., CRC Press, 2016. ⟨http://hbcponline.com.ezproxy.lib.vt.edu/faces/documents/04_02/04_02_0001.xhtml⟩.
[27] M.J.W. Jansen, Analysis of variance designs for model output, Comput. Phys. Commun. 117 (1999) 35–43, https://doi.org/10.1016/S0010-4655(98)00154-4.
[28] A. Saltelli, P. Annoni, I. Azzini, F. Campolongo, M. Ratto, S. Tarantola, Variance based sensitivity analysis of model output. Design and estimator for the total sensitivity index, Comput. Phys. Commun. 181 (2010) 259–270, https://doi.org/10.1016/j.cpc.2009.09.018.
[29] L. Song, NGPM – A NSGA-II program in Matlab v1.4 (version 1.6.0.0), MATLAB Central File Exchange, July 26, 2021.
[30] T.F. Coleman, Y. Li, An Interior trust region approach for nonlinear minimization subject to bounds, SIAM J. Optim. 6 (1996) 418–445, https://doi.org/10.1137/0806023.
[31] H. Dette, V.B. Melas, A. Pepelyshev, N. Strigul, Efficient design of experiments in the monod model, J. R. Stat. Soc. 65 (2003) 725–742. ⟨https://www.jstor.org/stable/3647548⟩.
[32] Y. He, Z. Xie, H. Zhang, W. Liebl, H. Toyama, F. Chen, Oxidative fermentation of acetic acid bacteria and its products, Front. Microbiol. 13 (2022), https://doi.org/10.3389/fmicb.2022.879246.